The Method to Curtail PV and Utilize it as Fast Frequency Response Study Case North Sulawesi and Gorontalo Power System

Arif Majiid Nusa Pratama[1,2], Muhammad Irfan Hashfi[2,3], Ido Fandy Dermawan[2],
Kevin Marojahan Banjar-Nahor[1], Fathin Saifur Rahman[1], Masayuki Watanabe[4], and Nanang Hariyanto[1]

[1]School of Electrical Engineering and Informatics, Institut Teknologi Bandung, Bandung, Indonesia
[2]PT PLN (Persero), Jakarta, Indonesia [3]Universitas Indonesia [4]Kyushu Institute of Technology
*Corresponding author: nusa.arif2@gmail.com

Abstract: Indonesia has committed to reducing greenhouse gas emissions and achieving maximum net zero emissions by 2060. To meet this commitment target, Indonesia possesses various renewable energy potentials, with photovoltaic (PV) systems emerging as one of the most popular generators. The North Sulawesi and Gorontalo regions boast significant PV potentials, reaching up to 20.81 GWp and 16.69 GWp respectively. However, PV penetration, characterized by its intermittent nature, presents a challenge in these regions due to their low system stiffness. Before the implementation of Battery Energy Storage Systems (BESS), PV curtailment served as a last resort during intermittencies that could disrupt system frequency. Curtailment involved several stages, including identifying PV locations requiring limitation using the Pearson correlation method, ensuring targeted curtailment by analyzing various variables influencing system frequency. Intermittent power variables from one of the PV sources significantly impact system frequency stability needed regulation through PV curtailment. The extent of curtailment required careful calculation to meet system demands, determined through data mining and correlation analysis between Power (P) and frequency (f). Using this correlation function, the amount of power to be curtailed could be determined through linear regression. Following PV curtailment, the curtailed power is utilized as Event Triggering Virtual Inertia, enhancing system reliability. Testing the Event Triggering Virtual Inertia method yielded satisfactory results, as evidenced by frequency stability, voltage, and generator rotor angle stability. These findings underscore the effectiveness of utilizing curtailed PV power as a means to bolster system reliability and stability.

Keywords: Photovoltaic Plant, PV Curtailment, Event Triggering Virtual Inertia, Data Mining

1. Introduction

By 2060, Indonesia aims to achieve net zero emissions (NZE)[1]. PV is a modern and sustainable energy alternative for reducing greenhouse gas emissions (GHG). According to [2], in order to attain NZE by 2060, photovoltaic (PV) must contribute at least one-third of total electricity output, with a capacity of 420 GW. Due to the intermittent nature of primary solar energy, this composition will have an impact on frequency stability, necessitating the inclusion of frequency regulation technology contributions such as battery energy storage systems (BESS)[3][4][5]. In addition to BESS technology, the curtail PV scheme [6][7] is an option. PV curtailment is required to limit PV operations and mitigate the impact of PV intermittency. Curtailment, in addition to mitigating PV intermittency, can be used as a system reserve or virtual inertia [8].

To address intermittency based on [9], various measures have been employed, including the gradual activation of the free governor and Automatic Generation Control (AGC). Additionally, curtailing PV output has been implemented to limit intermittent occurrences. Curtailment is necessary as the last effort under specific conditions: when PV intermittency causes frequency disturbances beyond normal operational limits, during system alert phases, and when the power plant Technical Minimum Load surpasses the system's load.

Using the history of the system strength index as a reference, one can calculate the amount of curtailment. The System Strength Index can be calculated from a single event or a series of sudden force outages that alter the frequency before it reaches the UFR setting limit. The two

Received: November 1sh, 2023. Accepted: March 26th, 2024
DOI: 10.15676/ijeei.2024.16.1.6

largest PV farms in the North Sulawesi and Gorontalo systems are Likupang PV (15 MWp AC) and Isimu PV (10 MW AC). With a peak daily system load of 330 MW and a total PV penetration of 25 MWp AC, PV contributes 7.58% to meeting system demand [9]. Despite the fact that PV penetration is only 7.58%, this circumstance affects system frequency stability. This is due to the system strength index in 2022 being just 22.32 MW/Hz [10]. The standard frequency control range of the Indonesian electricity network is 49.80 Hz - 50.20 Hz or + 0.2 Hz from 50 Hz [11]. Based on these circumstances, the system can only accept PV intermittency ranging from 4.64 MW to 9.29 MW while maintaining the normal operating frequency range of + 0.2 Hz. To achieve the desired normal frequency operation, the following flowchart is utilized:

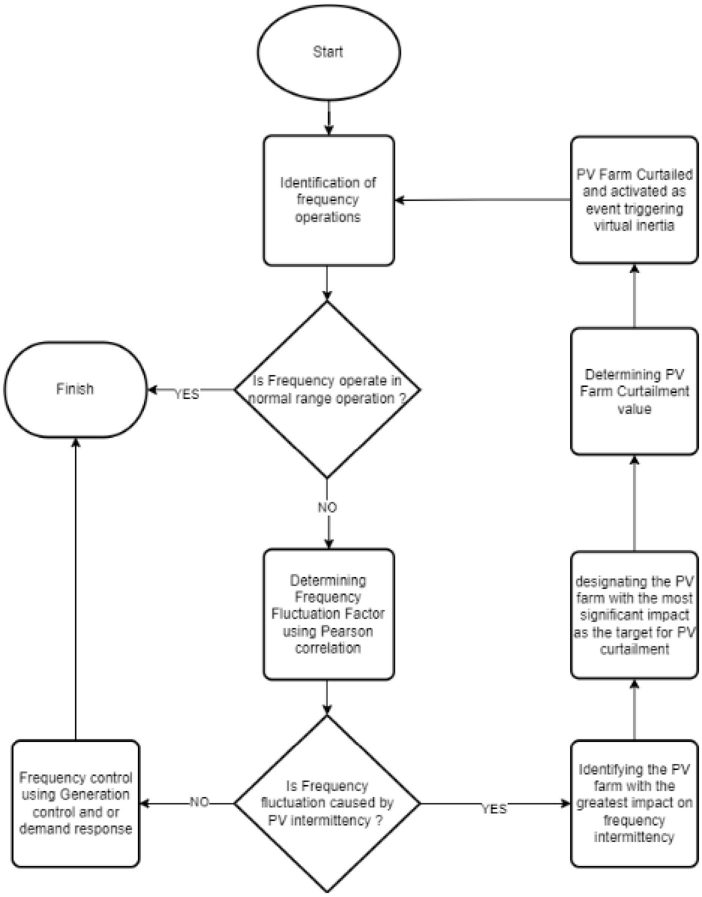

Fig. 1. Flowchart of curtailment method

To address the challenges of the PV condition without BESS, it's essential to employ the curtailment PV method based on Fig. 1. The flowchart provides instructions starting from the identification of whether the system frequency is within the normal operating range. If the frequency condition is found to be outside the normal limits due to PV intermittency, identification is required to determine which PV farm has the greatest impact on the stability of the system frequency operation. The PV farm with the greatest impact will be targeted for curtailment. The magnitude of curtailment will be determined based on the historical data of the last hour for that day, to find the function of linear regression which will be used as a reference for curtailment calculations. After curtailment is implemented, the system frequency conditions are monitored again.

This paper is structured into several sections. Section (II) focuses on Data Mining and Mapping variables influencing the system frequency, utilizing the Data Science Trajectory

(DST) Method. The primary variables under scrutiny include the system load, Likupang PV power, and Isimu PV power. The objective is to identify which of these variables has the most substantial correlation with system frequency changes. Those with the highest correlation are then targeted for adjustments to mitigate the impact on system frequency.
Upon determining which PV farm significantly influences frequency alterations, section (III) delves into ascertaining the curtailment value. This determination requires the latest operational history data, which reveals the relationship between PV power changes and system frequency fluctuations. The derived curtailment value is subsequently tested in section (IV) through Simulation and Experiment. Simulations are conducted in the DIgSILENT application, where the curtailment value is input to assess its impact pre and post-curtailment. Following the simulation, experimental testing is executed in the North Sulawesi and Gorontalo systems to evaluate the curtailment's effect on system frequency stability. The simulation to activating the curtailed energy as virtual inertia will be shown in (V) Event Triggering Virtual Inertia, Detailed insights from these tests are elaborated upon in section (VI) Discussion, culminating in the (VII) Conclusion.

2. Data Mining and Variable Mapping

A. Data Science Trajectory Method

The CRoss-Industry Standard Process for Data Mining (CRISP-DM) is a guidance method for conducting data mining projects[12]. This paper will use CRISP-DM enhancement, namely the Data Science Trajectory (DST) Model. The DST model offers a comprehensive framework for data science projects, integrating both exploratory and goal-directed activities. While it encompasses the outer circle of exploratory tasks and the core data management activities, at its heart lies the CRISP-DM process, a recognized standard in data mining for over two decades[13]. The DST model not only retains the foundational elements of CRISP-DM but also enhances it by introducing new activities essential for modern data science projects, such as data source exploration, goal setting, and result interpretation in relation to business objectives. This revamped model acknowledges the limitations of the original CRISP-DM in today's diverse data science landscape, offering greater flexibility by identifying various trajectories and practices in data science. Furthermore, the DST model can be adapted to different organizational contexts, serving as a template for project managers to tailor their data science workflows [13][14].

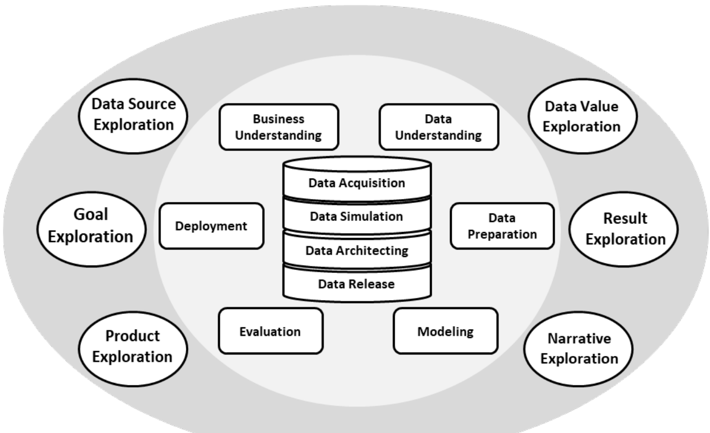

Fig. 2.The DST map [13]

From the DST map illustrated in Fig. 2, the systematic approach to data mining on variables is delineated as flowchart in Fig. 3:

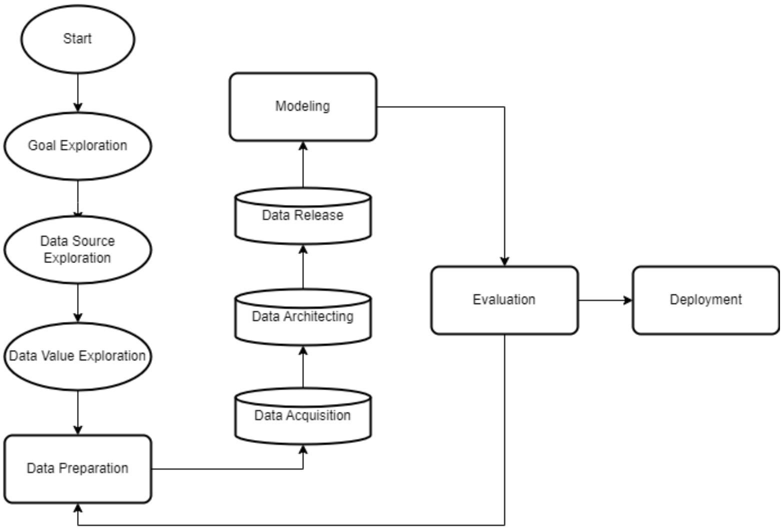

Fig. 3. DST Flowchart

In Fig. 3 shows the flowchart of DST map to determine the PV farm that will be curtailed and the PV curtailment equation.

I. Exploration activities:

a. Goal Exploration: The primary aim here is to uncover correlations between variables that influence system frequency changes. This includes factors like demand fluctuations and PV intermittency. The goal is to pinpoint precise interventions needed to keep the frequency within its standard operational range.

b. Data Source Exploration: This step involves identifying potential data sources. For this study, data has been sourced directly from the SCADA master station.

c. Data Value Exploration: Once the sources are identified, a meticulous search is undertaken to ensure the comprehensiveness of the variable values. The data extracted encompasses frequency values, customer load metrics, PV power readings, equipment status, and specific sensor measurements (like irradiance and temperature) from each PV Farm.

2. Data Preparation: This phase is dedicated to data sourcing and value extraction. It sets the stage for subsequent data management tasks.

3. Data Management Activities:

a. Data Acquisition: At this juncture, data pertaining to frequency, customer load, PV power, and sensor readings (covering irradiance and temperature) from each PV farm are gathered. These are collected at one-second intervals, spanning a historical timeframe of 1-2 hours. This approach assumes consistent parameters and responses from the operating generators during this period.

b. Data Architecting: The amassed data undergoes a filtration process to take out anomalies and ensure equipment status is on the standard. Post-filtration, the data is processed to convert meter readings into a format that showcases the magnitude of measurement variations over time.

c. Data Release: The refined data from the previous step is then modeled and subjected to evaluation.

4. Modeling: At this stage, the data, which highlights the impact of variable fluctuations on frequency changes, is scrutinized using the Pearson correlation method. This helps in identifying the most influential variables causing frequency alterations. Based on these variables, data processing is executed to derive a function that relates power shifts to frequency shifts. This

function serves as a benchmark for modulating PV power, ensuring that frequency oscillations remain within the acceptable operational spectrum.
5. Evaluation: The derived function for ascertaining curtailment undergoes rigorous testing via simulations and hands-on experiments.
6. Deployment: Post-evaluation, the curtailment determination function is ready for practical application.

B. Variable Correlation

Data analysis is performed using Pearson correlation in the modeling step, according to the DST flow. Pearson correlation is a method for measuring the linear strength of the relationship between two continuous variables [15][16]. Pearson correlation is calculated by determining the variance (var), covariance (cov), and standard deviation (SD) values.,

$$var(x, y) = \frac{\sum_{i=1}^{n}(x_i - \bar{x})}{n-1} \quad (1)$$

Variance measures the average squared deviation of each data point from the mean. For a dataset of 'n' values. x_i is the value of variant x, $\bar{x}$ is the mean of the data set for variant x Then, The standard deviation is the square root of the variance and measures the spread of data points around the mean, as follows:

$$SD(x) = \sqrt{var(x)} \quad (2)$$

Covariance measures the degree to which two variables change together. It's calculated as the average of the products of deviations from the mean for X and Y. Calculated using the following formula,

$$cov(x, y) = \frac{\sum_{i=1}^{n}(x_i - \bar{x})(y_i - \bar{y})}{n-1} \quad (3)$$

From equations (2) and (3), the calculation continues with the calculation of the Pearson correlation coefficient (r):

$$r = \frac{cov(x,y)}{SD(x).SD(y)} \quad (4)$$

These calculations help quantify the relationship between two variables in terms of direction and strength. The correlation coefficient provides valuable insights into how changes in one variable may relate to changes in another variable

A. Data Mining Result

The Likupang PV and Isimu PV locations are situated in different areas, resulting in varying irradiation conditions. This disparity is not solely due to sunlight irradiation but is also influenced by cloud cover, leading to different intermittency patterns between Likupang PV and Isimu PV. Thus, it is imperative to map the variables influencing system frequency changes for both PV farms. PV installations exhibiting higher correlations will be targeted for curtailment implementation.

The sampling duration chosen is 1 hour, with data collected per second. This selection aims to achieve relatively consistent conditions for both generation and consumer components of the system. Consequently, variations in generation and consumer variables will have relatively the same frequency response to the PV intermittency. Changes in generation composition, including the number of operating units and generated power, will notably affect frequency regulation, especially during PV intermittency events. Comparing generation conditions between morning and afternoon reveals a higher proportion of generation during the latter due to increased system load. This influences the generation units' responsiveness during intermittent events in the power system. Moreover, the activation of Automatic Generation Control (AGC) in each generator entails specific minimum and maximum loading requirements, as well as different AGC operational ranges. The availability of spinning reserves in generators further affects their responses. Therefore, considerations regarding generator loading, AGC, and spinning reserve availability are crucial when selecting data sampling periods to ensure consistent generation conditions during PV intermittency responses.

Data acquisition from the results of data mining on January 13, 2023, at 12:00-13:00, with each second-time interval, can be seen in Fig. 4,

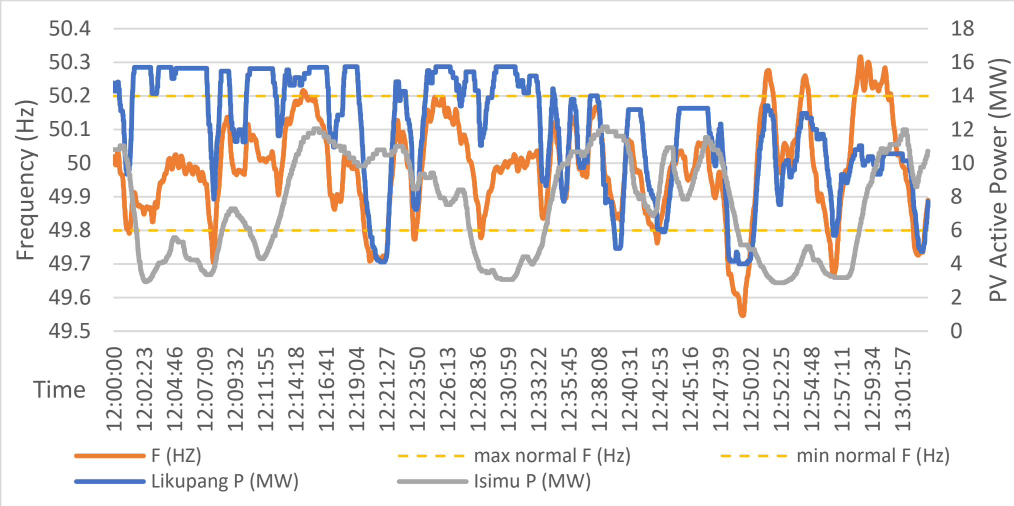

Fig. 4. The frequency graph and PV graph show a violation of the frequency's normal operating limitations due to PV intermittency.

Fig. 4 solely depicts the PV power measurement graph and the system frequency. This graph depicts the effect of PV intermittency on frequency. According to the statistics, the highest power change of Likupang PV was 11.62 MW in 2 minutes at 12:20, causing the frequency to decrease to 49.71 Hz. Table.1 shows the magnitude of the correlation between frequency changes caused by variable changes.

Table 1. Pearson Correlation Coefficient of Variables

	F (HZ)	*Likupang P (MW)*	*Likupang SUNR*	*Likupang TEMP*	*Isimu P (MW)*	*Isimu SUNR*	*Isimu TEMP*	*Demand (MW)*
F (HZ)	1.00000							
Likupang P (MW)	0.46762	1.00000						
Likupang SUNR	0.07111	0.10055	1.00000					
Likupang TEMP	0.00602	0.00745	0.01489	1.00000				
Isimu P (MW)	0.11730	0.03233	-0.00984	0.01902	1.00000			
Isimu SUNR	-0.01420	-0.00091	0.04088	-0.01746	0.04592	1.00000		
Isimu TEMP	-0.01982	0.00644	0.02391	-0.03715	-0.01795	0.52898	1.00000	
Demand (MW)	0.12138	0.34288	0.05678	-0.00210	0.12640	0.01885	-0.00133	1.00000

Table I shows the relationship between the magnitude of power variations in PV (ΔP) and changes in system frequency (ΔF). The power change at Likupang PV (ΔP) has the strongest Pearson correlation coefficient to the change in frequency (ΔF) with a correlation value of 46.76. Likupang PV can be targeted for curtailment based on this information.

3. Determine The Curtailment Value

The data modeling process includes determining the curtailment size. After calculating the PV target for curtailment, the curtailment equation must be determined. From data in Fig. 3 the correlation analysis is needed to determine the curtailment value. A linear function from a set of correlation data on the $P(t_1\text{-}t_0)$ and $F(t_1\text{-}t_0)$ per second graph can be used in this curtailment equation. The distribution of $P(t_1\text{-}t_0)$ called ΔP on the y-axis and $F(t_1\text{-}t_0)$ called ΔF on the x-axis may be observed in Fig. 5. Filtering is required to improve the accuracy of the curtailment equation.:

1. When ΔP from Likupang PV does not change, the resulting ΔF is not caused by ΔP from Likupang PV.
2. Changes in f (Hz) and P (MW) must be aligned; if f+, then P+, and vice versa.
3. Data were collected when 49.8 (Hz) > f (Hz) > 50.2 (Hz).

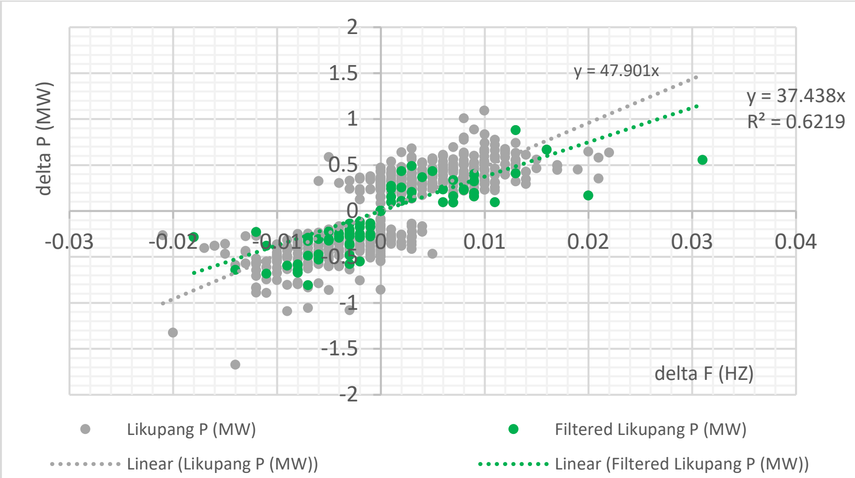

Fig. 5. $P(t_1\text{-}t_0)$ and $F(t_1\text{-}t_0)$ Correlation chart with linear curtailment equation, grey dot before filtering data and green dot after filtering data

The Curtailment equation can be derived from the linear function as follows:

$$y = 37.438x \qquad (5)$$

Where x is the maximum intended frequency operating range value and y is the maximum PV operation that will become the operational limit. The R^2 value is 62.24%. In this case, the maximum permissible intermittency of Likupang PV is 7.49 MWp in order to match the standard frequency setting of ±0.2 Hz.

$$P_{max} = y\,.(100\% + (100\% - Max\ Intermitency\%) \qquad (6)$$

The maximum permissible PV operation is $P_{max,}$ while the greatest power intermittency that the system can accept is y. According to the hourly data, the intermittency from the MAP to the minimum value is roughly 70%. The P_{max} value is 9.7 MW.

It's acknowledged that an R-squared (R^2) value of 0.62 may not initially meet the desired accuracy level, although a higher value is preferred for enhanced precision. It's important to note that within the fluctuations of the system frequency, various factors besides PV intermittency contribute, such as changes in system load and generator controls. Hence, while an R-squared correlation coefficient of 0.62 may indicate a moderate level of association between the variables in the linear regression model, it needs to be validated through simulation and experimentation

4. Curtailment Test

The testing is performed in two ways: through DIgSILENT simulation and through experimentation. The influence of intermittency is observed in the DIgSILENT simulation tests when power loss happens from its Maximum Available Power (MAP) after curtailment. Following the simulation test, a real-time experiment in the power system will be performed.

A. Simulation

The North Sulawesi and Gorontalo power systems were modeled in the DIgSILENT simulation using real-time conditions. It was designed as a negative load to simulate PV power intermittency. The simulation was divided into two scenarios: scenario I, in which PV was running normally, and scenario II, in which PV had been curtailed.

1. Scenario I, with a maximum PV power reading from the metering system of 15.74 MW, witnessed an intermittency drop of up to 11.62 MW, or 73.79% of the MAP.
2. Scenario II, according to the curtailment function, limits the PV to a MAP of 9.7 MW, with a power loss of 7.08 MW assuming 73.79% intermittency.

The first scenario (scenario I) will be the base condition, this base condition is simulated based on real events. This will also help validate the simulation condition already similar to the real event. Observing frequency response owing to intermittency in both circumstances using RMS/EMT Simulation. The simulation lasts 250 seconds and is based on the conditions on January 13, 2023, at 12:20 p.m. In real-time conditions the power drop down 11.62 MW causing the system frequency to drop to 49.71 Hz

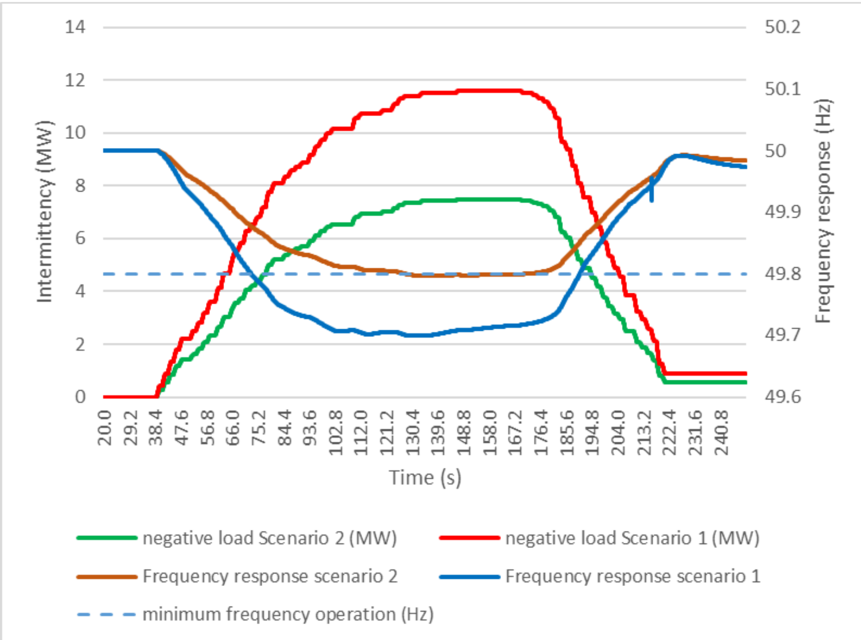

Fig. 6. When there is a decrease in PV power before curtailment, the red line represents PV as a negative load, the blue line is the frequency response before PV curtailment, the green line is the PV power decrease as a negative load after curtailment, and the brown line is the frequency response after PV curtailment.

According to the simulation findings presented in Fig.6, the frequency reached as low as 49.71 Hz before the curtailment, showing that the intermittency influence led the frequency to operate outside the normal limit (± 0.2 Hz), this simulation shows the base condition for the simulation already similar to the real condition. The impact of intermittency 7.49 MW on the frequency only caused it to decrease to 49.8 Hz after the curtailment, suggesting that the frequency was able to continue regular operation after the curtailment. This will be followed by power system experiments based on the results of the DIgSILENT simulation.

B. Experiment

The experiment began at 13:07 on January 13th, 2023, with an instruction from the control center to reduce Likupang PV MAP to 9.59 MW.

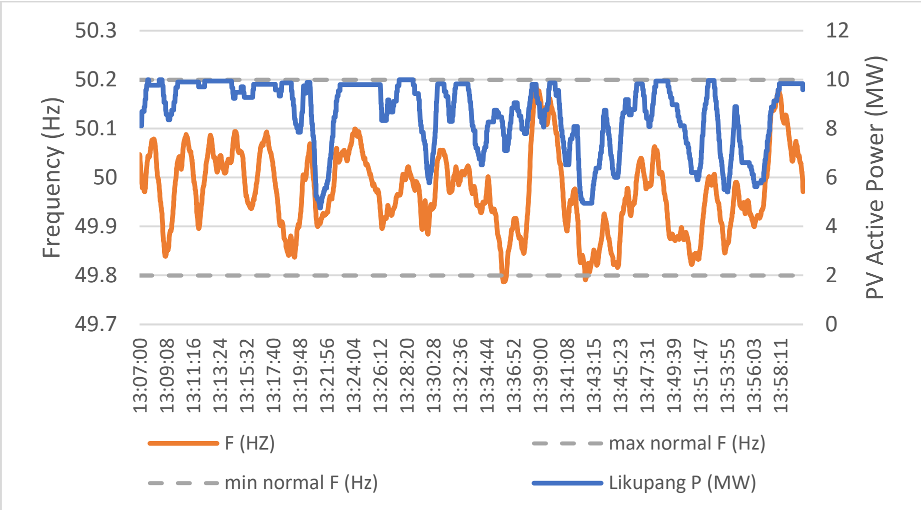

Fig. 7. After curtailment, the frequency running under normal conditions (± 0.2 Hz)

As shown in Fig. 7, the frequency deviation satisfies the intended normal operating level of ±0.2 Hz under curtailment. This implies that the curtailment technique and function utilized are consistent with the desired outcome. During 13.21 and 13.42 the P of Likupang PV decreased until 4.7 MW close to the previews event before the curtailment which is 4.1 MW, succeeded in avoiding the under frequency condition (<49.8Hz).

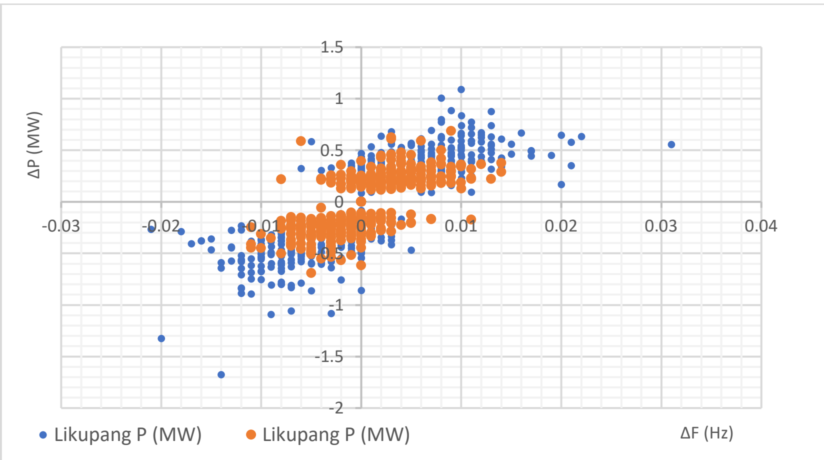

Fig. 8. The $P(t_1\text{-}t_0)$ and $F(t_1\text{-}t_0)$ correlation chart and linear curtailment equation are shown, with the blue dot indicating the correlation before curtailment and the orange dot indicating the correlation after curtailment

In Fig. 8 depicts the change in the $P(t_1\text{-}t_0)$ and $F(t_1\text{-}t_0)$ correlation graph following the implementation of Likupang PV curtailment. The influence of Likupang PV power change (ΔP) on frequency change (ΔF) is found to decrease. The blue dots represent the association between frequency change and Likupang PV power change before the curtailment, whereas the orange dots represent the same relationship after the curtailment. The distribution of orange dots is smaller than that of blue dots, showing that the impact of PV intermittency on system frequency has been reduced.

Table 2. Pearson Correlation Coefficient of Variables After Likupang PV Curtailment

	F (HZ)	*Likupang P (MW)*	*Likupang SUNR*	*Likupang TEMP*	*Isimu P (MW)*	*Isimu SUNR*	*Isimu TEMP*	*Demand (MW)*
F (HZ)	1.00000							
Likupang P (MW)	0.32164	1.00000						
Likupang SUNR	0.06153	0.13522	1.00000					
Likupang TEMP	0.01286	-0.00713	-0.01601	1.00000				
Isimu P (MW)	0.24291	0.03806	-0.02211	0.01146	1.00000			
Isimu SUNR	0.04858	0.04578	0.01705	0.01082	0.08776	1.00000		
Isimu TEMP	-0.02615	-0.01537	0.03185	-0.01283	-0.04480	-0.02659	1.00000	
Demand (MW)	0.05176	0.24379	0.00396	-0.01695	0.21425	0.04000	-0.00999	1.00000

The correlation value between frequency change and Likupang PV power change reduced from 46.76% to 32.16% in Table 2. This decrease in correlation value suggests that the impact of Likupang PV intermittency on system frequency has decreased.

Through the conducted simulation and experimentation, the efficacy of the proposed curtailment method is evaluated. The results demonstrate satisfactory outcomes, wherein the actual frequency operation aligns with the targeted frequency fluctuation limitations of ±0.2 Hz from the nominal frequency of 50 Hz. This validation process confirms that despite the moderate correlation coefficient, the linear regression function derived from the R-squared value of 0.62 yields accurate predictions and effectively addresses the frequency fluctuation issue within acceptable limits.

By emphasizing the validation of the proposed method through simulation and experimentation, the study ensures that the derived linear regression function can be confidently utilized for prediction purposes, substantiating its practical applicability and reliability in real-world scenarios.

In assessing the accuracy of the curtailment method, it is crucial to examine its effectiveness in achieving the desired frequency targets. By evaluating the results of PV curtailment, it is observed that the minimum frequency attained is 49.726 Hz, while the lowest targeted frequency fluctuation is set at 49.800 Hz. Calculating the percentage success rate reveals an impressive outcome of 99.85%. This high level of success underscores the efficacy and reliability of the curtailment strategy in maintaining the system frequency within acceptable limits. Such a precise alignment between the actual frequency and the targeted fluctuation range demonstrates the method's ability to effectively mitigate frequency deviations caused by PV intermittency. Consequently, this validation metric further reinforces the confidence in the proposed curtailment equation and justifies its implementation without the need for additional simulation validation

5. Event Triggering Virtual Inertia

The study was carried out by simulating the contribution of spinning reserve from PV to the system when the frequency decreased to a certain point. The spinning reserve availability could be seen from the PV Maximum Power Point (MPP) forecast due the PV curtailment operations. The simulation will test some different under frequency point, to figure the result of each frequency setting. In the testing results with a scenario of PV curtailment of 10 MW at Likupang PV, where the available PV MPP is 15 MW, under these conditions, Likupang PV holds a reserve of 5 MW. These reserves from the PV function as event triggering virtual inertia. In this simulation, an event disturbance occurs at unit 2 of the Sulut CPP, with an outage power of 26 MW. The simulation compares the event triggering virtual inertia (ETVI) at several frequency trigger points:

1. Curtailment release at a frequency of 49.60 Hz (ETVI 49.6 Hz)
2. Curtailment release at a frequency of 49.50 Hz (ETVI 49.5 Hz)
3. Curtailment release at a frequency of 49.40 Hz (ETVI 49.4 Hz)
4. Curtailment release at a frequency of 49.30 Hz (ETVI 49.3 Hz)

For each ETVI event, additional logic is applied by considering the conditions of PV curtailment ($P_{curtailment}$) and real Power (P_{real}) from the PV. If $P_{real} < P_{curtailment}$, the ETVI will not be activated because the PV lacks the power reserves to respond. All of the logic using the "and gate"

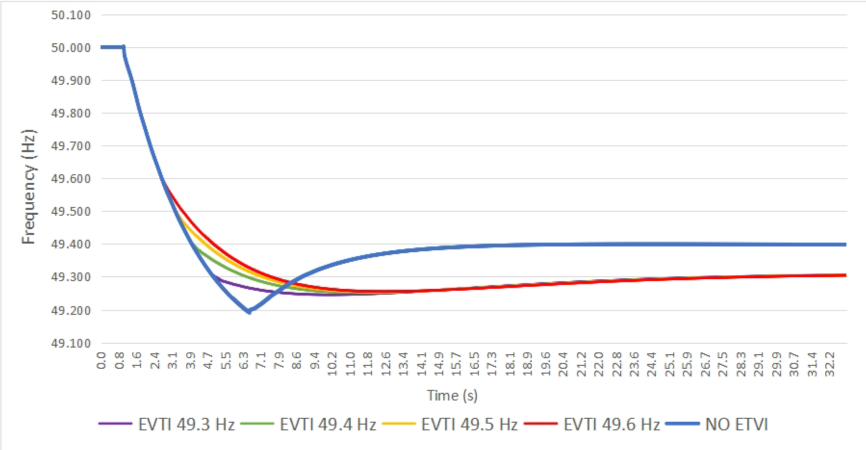

Fig. 9 Frequency response for every ETVI scenario and without ETVI scheme

In Fig. 9 the frequency response for each frequency setting for the Event Triggering Virtual Inertia can be observed. The frequency condition during steady-state after the response from Likupang PV at the 32nd second of simulation indicates similar results, with the frequency being at 49.31 Hz. During the activation of ETVI in the early second the difference the frequency ETVI activated at 49.60 Hz is the farthest from UFR phase 1 setting (49.20 Hz), in other hand the purple line ETVI 49.30 Hz is the closest to UFR phase 1 setting (49.20 Hz).

The voltage conditions at the substations displayed represent each subsystem. To determine the voltage conditions in each simulated scenario, the voltage response is monitored in each subsystem. Subsystem 1 and subsystem 2 are located in North Sulawesi. Subsystem 1 consists of a 66 kV system and partly a 150 kV system, while subsystem 2 is a 150 kV system located in North Sulawesi. Subsystem 3 is a 150 kV system in Gorontalo.

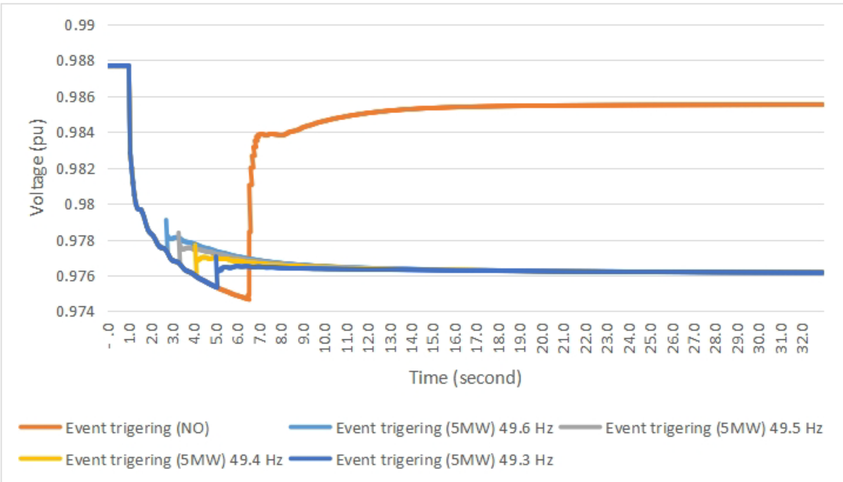

Fig. 10 Likupang Substation voltage (subsistem1)

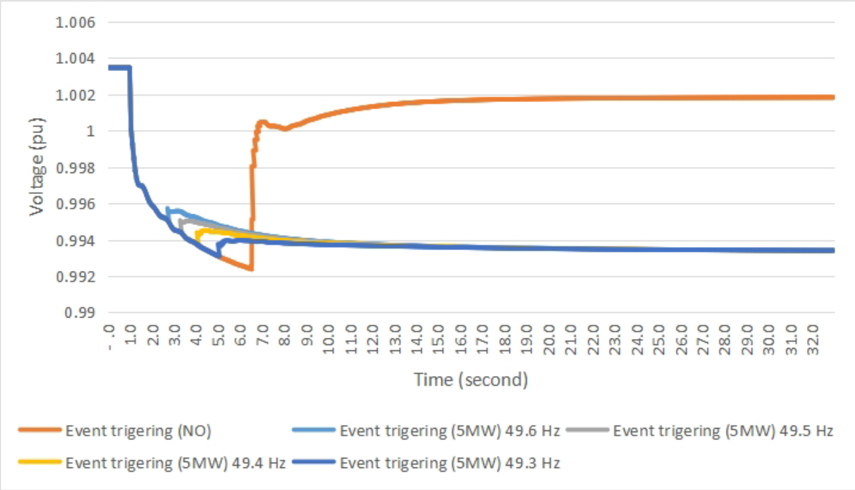

Fig. 11 Amurang substation voltage (subsistem 2)

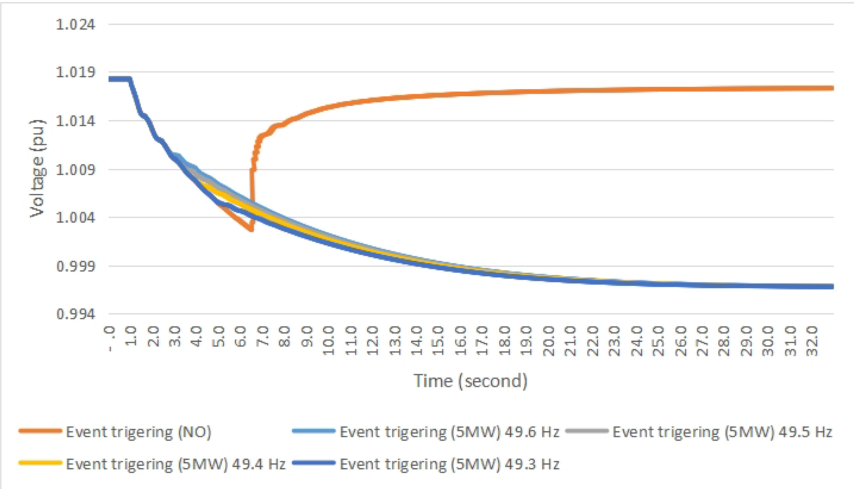

Fig. 12 Isimu substation voltage (subsistem 3)

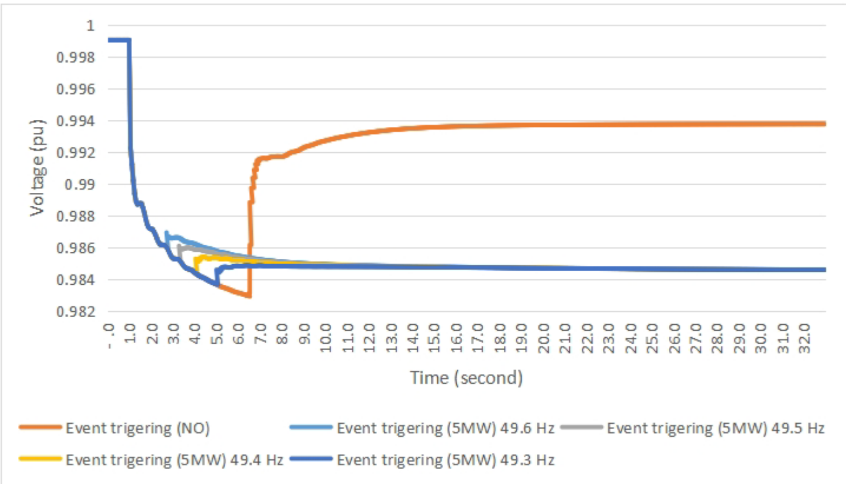

Fig. 13 Sulut 3 substation the closet from power plant outage

From Fig. 10, Fig. 11, Fig. 12, and Fig. 13, it can be observed that the highest voltage fluctuations occur at the Sulut 3 substation due to its proximity to the location of the generating unit experiencing an outage. Meanwhile, at the Isimu substation, voltage changes are not significantly affected due to its distant location from the generating unit disturbance and Likupang PV. At the location closest to the generating unit disturbance, it can be seen from the graphs that the ETVI scheme can reduce the lowest voltage points. The faster the contribution from the ETVI, the better the voltage conditions during transient occurrences.

The active power generated by the PV curtailment plays a crucial role in voltage regulation within the system. When the curtailed active power from the PV system is released, it contributes to the overall active power supply within the system. This additional active power can offset the contributions from other generators, thereby affecting the reactive power flow in the system.

In the specific scenario described, the release of active power from the PV curtailment enables other generators to supply reactive power to compensate for the reactive power loss from CPP Sulut 3 unit 2. This compensation helps stabilize the voltage levels across the system, particularly in substations closer to CPP Sulut 3. As a result, scenarios involving ETVI events tend to exhibit improved voltage conditions due to the synergistic effects of active and reactive power interactions.

In essence, the active power contribution from the released PV curtailment facilitates a more balanced power supply, allowing for efficient reactive power exchange among generators. This, in turn, leads to better voltage regulation and stability, particularly in areas directly impacted by the outage of CPP Sulut 3 unit 2.

Observing the rotor angle ensures that the generators are in synchronous condition during disturbances and when the ETVI scheme is operational. From the simulation results, it is evident that all generator units observed in each subsystem can follow the changes occurring in the system. The operational overview of generators in each subsystem can be seen in the following figures.

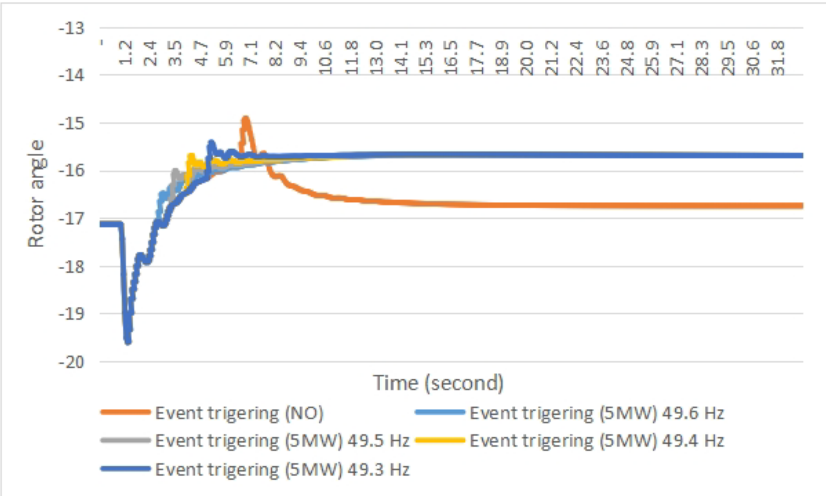

Fig. 14 Hydro power plant Tanggari II unit 1 rotor angle the closest power plant form Likupang PV

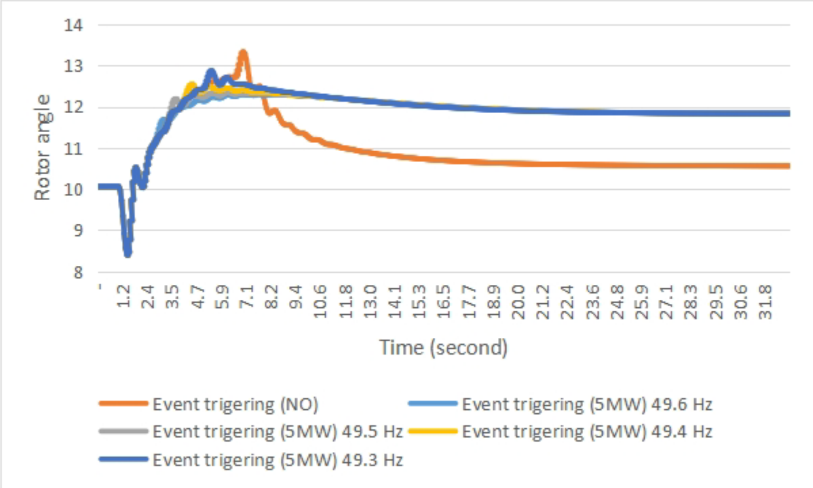

Fig. 15 Leasing Coal power plant Amurang unit 1 rotor angle

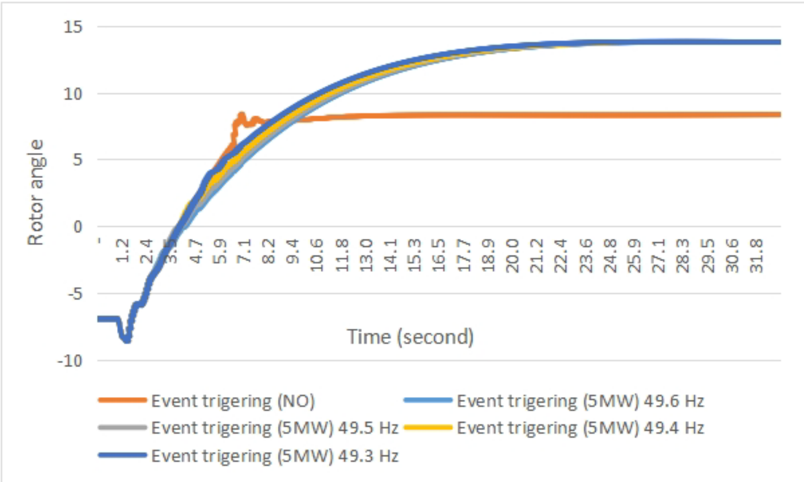

Fig. 16 Gas power plant Maleo unit 1 rotor angle

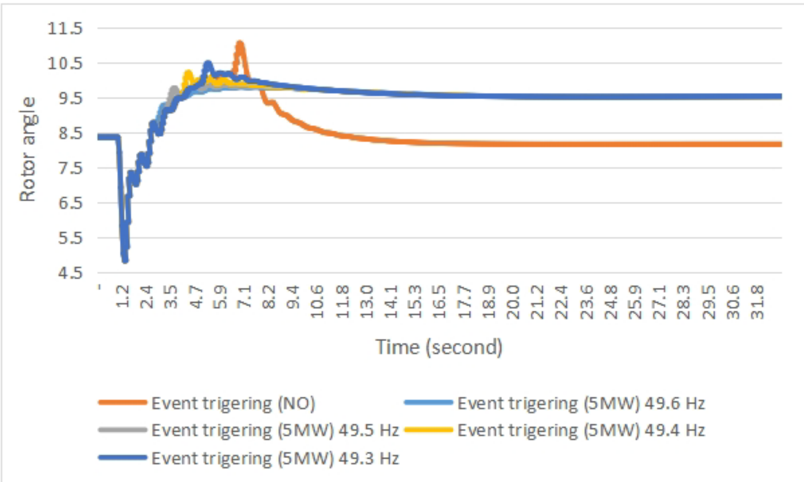

Fig. 17 Power plant Sulut 3 unit 1 rotor angle

In Fig. 14, Fig. 15, and Fig. 16, graphs represent each power plant unit representing subsystems. Fig. 17 provides an overview of the rotor angles in each scenario at locations close to the power plant outage. Fig. 14 showing the nearest power plant from Likupang PV. From the simulation results, the rotor angles demonstrate satisfactory outcomes because the ETVI scenarios do not encounter obstacles in responding to frequency drops caused by power plant disturbances.

The simulation not only from frequency but also the voltage and rotor angle. To find the best results these criteria are sorted :

1. The highest frequency nadir point.
2. The frequency stability point closest to 50 Hz.
3. The minimum voltage approaching 1 per unit (pu).
4. The lowest transient rotor angle.

The main objective of ETVI is to ensure that the system avoids UFR when a conventional generator experiences an outage. Thus, frequency criterion becomes the primary focus. System reliability criteria from the frequency perspective are determined by identifying the lowest frequency point and the steady-state frequency point closest to 50 Hz. Next is the category of minimum voltage occurring during transient conditions, where closer to 1 pu indicates better voltage. Meanwhile, transient rotor angle serves as an additional factor to ensure no generators experience out-of-step conditions, and the rotor angle with the lowest fluctuation during transient conditions is the desired value.

Table 3 Scenario Simulation Ranking from left as the best result

Scenario			EVTI 49.6 Hz	EVTI 49.5 Hz	EVTI 49.4 Hz	EVTI 49.3 Hz	NO ETVI
Frequency nadir point		Hz	49,2551	49,2541	49,2520	49,2453	49,1902
Last Frequency		Hz	49,3045	49,3047	49,3050	49,3053	49,3983
UFR		MW	0,0000	0,0000	0,0000	0,0000	16,0755
Minimum Voltage	Sulut3	pu	0,9846	0,9846	0,9844	0,9837	0,9829
	Likupang	pu	0,9762	0,9762	0,9760	0,9753	0,9747
	Amurang	pu	0,9934	0,9934	0,9934	0,9931	0,9924
	Isimu	pu	0,9968	0,9968	0,9968	0,9968	1,0026
Maximum Rotor angle	HPP Tanggari II #1	degree	(15,6793)	(15,6790)	(15,6782)	(15,4162)	(14,9095)
	CPP Amurang Leasing #1	degree	12,2989	12,3435	12,5409	12,8711	13,3308
	GPP Maleo #1	degree	13,8078	13,8090	13,8116	13,8182	8,3972
	CPP Sulut 3 #1	degree	9,7927	9,8637	10,2098	10,4844	11,0581

As observed, the simulation ranking of ETVI in Table 3 indicates the ranking according to the specified parameters. Therefore, the ETVI scenario with the 49.6 Hz setting is considered the best scenario. Although some parameters such as frequency and voltage have nearly identical results during steady state. When compared to operating the system without ETVI, the parameters of frequency, voltage, and rotor angle in steady-state conditions after first stage UFR operation indicate better results, however resulting in a customer outage of 16 MW.

5. Discussion

The PV on-grid system in North Sulawesi and Gorontalo operates without batteries, causing the system frequency to feel the impact of intermittency. To achieve this, PV control via maximum available power (MAP) limiting is required. MAP PV curtailment occurs at the end of the process when all generators have responded via primary and secondary control. As a result, PV curtailment was adopted as a last resort in this investigation. This is done because while reducing PV, the take-or-pay (TOP) cost incurred by the PV Independent Power Plant (IPP) must be taken into account.

The distribution and correlation value of the correlation between $P(t_1\text{-}t_0)$ PV and $F(t_1\text{-}t_0)$ in the system frequency is less than 60% due to the influence of the dead band. As a result, if the frequency remains below the dead band setting, the generator will not respond. The distribution tends to broaden from its linear line, as seen in the correlation graphs in Figs. 3 and 6. For example, when the power in Likupang PV changes by 0.5 MW, the frequency can shift from 0.002 Hz to 0.03 Hz. A 0.03 Hz frequency shift occurred in this data, in addition to the influence of other variables, which also occurred when the frequency was below the dead band setting, indicating that a little adjustment can alter the system frequency. Aside from the influence of other variables, a frequency change of only 0.002 Hz happened after the frequency had operated past the dead band setting, so the generator responded directly.

The outcomes of the simulation and experiment of curtailment method are the same. Limiting PV operation reduces intermittency, allowing the system frequency to remain within the usual operating frequency range. The curtailment approach was tested in this study using modeling and experiments. The simulation step can be avoided to reduce the time required to make real-time decisions.

Utilizing curtailment as fast frequency response with a virtual inertia event triggering scheme from simulation results is feasible. The simulation results for voltage indicate that the voltage conditions during transient and steady-state phases remain within the normal operating limits. In the simulation of rotor angles, the generators exhibit stable conditions, with no generators experiencing out-of-sync conditions. In each frequency setting scenario for activating spinning reserves, there is no frequency decrease touching 49.20 Hz, thereby preventing UFR occurrences. The optimal frequency setting in terms of frequency reduction, voltage stability, and rotor angle stability is observed at the frequency setting of 49.60 Hz. In implementation, adjustments can be made to the settings if, upon operational evaluation, the frequency settings for ETVI can still be lowered to widen the frequency control gap before ETVI is activated.

6. Conclusion

In addition to BESS technology, PV curtailment can help to preserve system frequency stability. Making judgments requires data mining and then determining the degree of curtailment using the Pearson correlation coefficient to find which PV farm will be curtailed. The curtailment value can be determined from the linear $P(t_1\text{-}t_0)$ and $F(t_1\text{-}t_0)$ per second equation. Curtailment can then be targeted to match the needs of the system based on the historical condition. The utilization of curtailment as a fast frequency response with the event triggering virtual inertia method can be implemented. ETVI settings based on ranking from frequency, voltage, and rotor angle scores indicate that the 49.6 Hz setting is the best, even though in steady-state conditions, each ETVI setting yields the same result.

7. References

[1]. Iea, "Peta Jalan Menuju Emisi Nol Bersih pada Sektor Energi di Indonesia," pp. 1–14, 2022, [Online]. Available: www.iea.org/t&c/.

[2]. IESR, "Indonesia Energy Transition Outlook 2023: Tracking Progress of Energy Transition in Indonesia: Pursuing Energy Security in the Time of Transition," 2021. [Online]. Available: www.irena.org.

[3]. T. Kerdphol, F. S. Rahman, M. Watanabe, and Y. Mitani, “Robust Virtual Inertia Control of a Low Inertia Microgrid Considering Frequency Measurement Effects,” *IEEE Access*, vol. 7, pp. 57550–57560, 2019, doi: 10.1109/ACCESS.2019.2913042.
[4]. W. H. Tee, C. Kim Gan, J. B. Sardi, K. Azmi Baharin, and K. K. Kong, “Probabilistic sizing of battery energy storage system for solar photovoltaic output smoothing,” *PECon 2020 - 2020 IEEE Int. Conf. Power Energy*, pp. 350–355, 2020, doi: 10.1109/PECon48942.2020.9314438.
[5]. R. P. Sasmal, S. Sen, and A. Chakraborty, “Solar photovoltaic output smoothing: Using battery energy storage system,” *2016 Natl. Power Syst. Conf. NPSC 2016*, pp. 1–5, 2017, doi: 10.1109/NPSC.2016.7858894.
[6]. J. A. Azzolini, M. J. Reno, N. S. Gurule, and K. A. W. Horowitz, “Evaluating distributed PV curtailment using quasi-static time-series simulations,” *IEEE Open Access J. Power Energy*, vol. 8, pp. 365–376, 2021, doi: 10.1109/OAJPE.2021.3111821.
[7]. J. A. Azzolini and M. J. Reno, “Impact of Load Allocation and High Penetration PV Modeling on QSTS-Based Curtailment Studies,” in *IEEE Power and Energy Society General Meeting*, IEEE Computer Society, 2021. doi: 10.1109/PESGM46819.2021.9638101.
[8]. Q. Peng, Z. Tang, Y. Yang, T. Liu, and F. Blaabjerg, “Event-Triggering Virtual Inertia Control of PV Systems with Power Reserve,” *IEEE Trans. Ind. Appl.*, vol. 57, no. 4, pp. 4059–4070, Jul. 2021, doi: 10.1109/TIA.2021.3080227.
[9]. A. M. N. Pratama, M. I. Hashfi, R. O. G. Munthe, K. M. Banjar-Nahor, and N. Hariyanto, “Operational Road Map in North Sulawesi and Gorontalo Power Grid Considering the Intermittent Photovoltaic Penetration,” in *ICPERE 2022 - 5th International Conference on Power Engineering and Renewable Energy, Proceedings*, Institute of Electrical and Electronics Engineers Inc., 2022. doi: 10.1109/ICPERE56870.2022.10037323.
[10]. UP2B SIstem Minahasa, “EVALUASI OPERASI SISTEM SULUTGO TAHUN 2022,” 2023.
[11]. Kementerian ESDM, “Aturan Jaringan Sistem Tenaga Listrik (Grid Code),” *Menteri Energi dan Sumber Daya Miner. Republik Indones.*, no. 3, pp. 417–607, 2020, [Online]. Available: https://jdih.esdm.go.id/storage/document/PM ESDM No 20 Tahun 2020.pdf.
[12]. R. Wirth and J. Hipp, “CRISP-DM: towards a standard process model for data mining. Proceedings of the Fourth International Conference on the Practical Application of Knowledge Discovery and Data Mining, 29-39,” *Proc. Fourth Int. Conf. Pract. Appl. Knowl. Discov. Data Min.*, no. 24959, pp. 29–39, 2000, [Online]. Available: https://www.researchgate.net/publication/239585378_CRISPDM_Towards_a_standard_process_model_for_data_mining.
[13]. F. Martinez-Plumed *et al.*, “CRISP-DM Twenty Years Later: From Data Mining Processes to Data Science Trajectories,” *IEEE Trans. Knowl. Data Eng.*, vol. 33, no. 8, pp. 3048–3061, Aug. 2021, doi: 10.1109/TKDE.2019.2962680.
[14]. W. Y. Ayele, “Adapting CRISP-DM for idea mining a data mining process for generating ideas using a textual dataset,” *Int. J. Adv. Comput. Sci. Appl.*, vol. 11, no. 6, pp. 20–32, 2020, doi: 10.14569/IJACSA.2020.0110603.
[15]. J. Hauke and T. Kossowski, “Comparison of values of pearson’s and spearman’s correlation coefficients on the same sets of data,” *Quaest. Geogr.*, vol. 30, no. 2, pp. 87–93, Jun. 2011, doi: 10.2478/v10117-011-0021-1.
[16]. H. Xu and Y. Deng, “Dependent Evidence Combination Based on Shearman Coefficient and Pearson Coefficient,” *IEEE Access*, vol. 6, pp. 11634–11640, Dec. 2017, doi: 10.1109/ACCESS.2017.2783320.

Arif Majiid Nusa Pratama received a B.Sc. degree from the Electrical Power Engineering from Institut Teknologi Minaesa in 2017. He has a passionate interest in renewable energy, system planning, energy investment, HV-MV systems, stability studies, and dynamics made him participate in some scientific projects and research, especially on tackling Energy problems. He has experience as an HV-MV Power System Dispatcher, System Operation Planning, and System Planning Engineer in PLN. He is currently a PLN scholarship awardee at ITB, Bandung, Indonesia with a joint master research program at Kyushu Institute of Technology in Japan, to study Renewable Energy.

Muhammad Irfan Hashfi is an experienced and adaptable SCADA Engineer with expertise in PLC programming, automation, and SCADA systems. He holds a Bachelor's degree in Electronics Engineering from Institut Teknologi Bandung and is currently pursuing a Master's degree in Information Technology with a focus on Business Analytics at the Universitas Indonesia. With over 5 years of experience at PT PLN (Persero), he has excelled as an Assistant Engineer at SCADA and Master Station, contributing to the efficient regulation of the electricity system in North Sulawesi and Gorontalo Provinces. Irfan's work includes maintenance, troubleshooting, commissioning, integration, and tuning of SCADA systems, as well as expanding SCADA features and driving automation.

Ido Fandy Dermawan received a B.Sc degree in Physics Engineering from Gadjah Mada University in 2013. He has experience as an HV equipment maintenance engineer, Operation Control engineer, Planning & Evaluation engineer in PLN since 2015. He has an interest in energy management & renewable energy applications, especially hydrogen & fuel cells. He is currently a Planning & evaluation manager at PLN UP2B Minahasa. He is responsible for making daily, weekly, monthly & yearly planning documents & evaluation documents, especially for North Sulawesi & Gorontalo region.

Kevin Marojahan Banjar-Nahor was born in Bandar Lampung, Indonesia in 1993. He received a B.S. degree and an M.S. degree in Electrical Power Engineering from Institut Teknologi Bandung in 2013 and 2014, respectively. He conducted his PhD research at the Grenoble Electrical Engineering Laboratory and received his PhD degree in Electrical Engineering from Grenoble Alpes University in 2019. His field of interest includes power system planning and operation, power system and microgrid stability, and power system protection. He is actively involved in industrial collaborations and professional associations in the field of power systems in Indonesia. He was a visiting researcher at LAPLACE Laboratory in Toulouse, France in 2021. Currently, he is an assistant professor at the School of Electrical Engineering and Informatics, Institut Teknologi Bandung.

Fathin Saifur Rahman received a B.Sc. degree in electrical power engineering and an M.Sc. degree in electrical engineering from Institut Teknologi Bandung, Indonesia, in 2012 and 2013, respectively, and a Doctoral degree from Kyushu Institute of Technology, Japan, in 2019. He is currently an assistant professor at the School of Electrical Engineering and Informatics, Institut Teknologi Bandung, Indonesia. His research interests include power system stability, smart grid and clean energy, virtual inertia, and optimization in power systems.

Masayuki Watanabe Received the B.Sc., M.Sc., and D.Eng. degrees in electrical engineering from Osaka University, Japan, in 2001, 2002, and 2004, respectively. Since 2004, he has been with the Department of Electrical and Electronic Engineering, Kyushu Institute of Technology (Kyutech), Fukuoka, Japan, where he is currently an Associate Professor. He holds the PMU licensed patent. He has authored books/book chapters and over 100 journal/conference papers. His research interest includes the area of the analysis of power systems. He is also a member of the Institute of Electrical Engineers of Japan (IEEJ).

Nanang Hariyanto Finished His Graduate Program In Electrical Engineering At Bandung Institute of Technology in 1986 and then continued his research and education at TU BERLIN (Technische Universitaet Berlin), Germany, from 1991 until 1993. In 2010, he earned a Doctoral Degree in Electrical Engineering from the Bandung Institute of Technology. He became a lecturer in the Department of Electrical Engineering ITB in 1989. He has been the Head of the Electrical Power System Laboratory from 2012 until now. He was the Head of the Electrical Power Engineering Study Program from 2014 to 2017. He is a member of the IEEE Power Engineering Society and Industrial Application Society, CIRED, IATKI, and KAN. Some of his key studies and projects are Roadmap for Energy Losses of PLN Indonesia, Non-Site Nuclear Power Plant Feasibility Study, and Research of Dynamic Stability Studies for Sumatera Electrical Power System Interconnection. He has experience and expertise in all matters related to electrical power system engineering: stability, load flow, short circuit study, feasibility study, electrical power system planning, electrical power system evaluation, investigation, and assessment.